Magnetic circular dichroism in the *dd* excitation in the van der Waals magnet CrI_3 probed by resonant inelastic x-ray scattering

Anirudha Ghosh,[1,2] H. Johan M. Jönsson,[1,3] Deepak John Mukkattukavil,[1] Yaroslav Kvashnin,[1] Dibya Phuyal,[4] Patrik Thunström,[1] Marcus Agåker,[1,2] Alessandro Nicolaou,[5] Martin Jonak,[6] Rüdiger Klingeler,[6] M. Venkata Kamalakar,[1] Tapati Sarkar,[7] Alexander N. Vasiliev,[8,9,10] Sergei M. Butorin,[1] Olle Eriksson,[1,11] and Mahmoud Abdel-Hafiez[1,12,*]

[1]*Department of Physics and Astronomy, Uppsala University, Box 516, SE-751 20 Uppsala, Sweden*
[2]*MAX IV Laboratory, Lund University, P.O. Box 118, SE-22100 Lund, Sweden*
[3]*Asia Pacific Center for Theoretical Physics, Pohang 37673, Korea*
[4]*Department of Applied Physics, KTH Royal Institute of Technology, SE-106 91 Stockholm, Sweden*
[5]*Synchrotron SOLEIL, L'Orme des Merisiers, Saint-Aubin, BP48, F-91192 Gif-sur-Yvette, France*
[6]*Kirchhoff Institute of Physics, Heidelberg University, D-69120 Heidelberg, Germany*
[7]*Department of Materials Science and Engineering, Box 35, Uppsala University, SE-751 03 Uppsala, Sweden*
[8]*National University of Science and Technology "MISiS," Moscow 119049, Russia*
[9]*Lomonosov Moscow State University, Moscow 119991, Russia*
[10]*Ural Federal University, Ekaterinburg 620002, Russia*
[11]*School of Science and Technology, Örebro University, SE-701 82 Örebro, Sweden*
[12]*University of Doha for Science and Technology, P.O. Box 24449, Doha, Qatar*

(Received 18 January 2022; revised 10 February 2023; accepted 13 February 2023; published 24 March 2023)

We report on a combined experimental and theoretical study on CrI_3 single crystals by employing the polarization dependence of resonant inelastic x-ray scattering (RIXS). Our investigations reveal multiple Cr 3*d* orbital splitting (*dd* excitations) as well as magnetic dichroism (MD) in the RIXS spectra. The *dd* excitation energies are similar on the two sides of the ferromagnetic transition temperature, $T_C \sim 61$ K, although MD in RIXS is predominant at 0.4 T magnetic field below T_C. This demonstrates that the ferromagnetic superexchange interaction that is responsible for the interatomic exchange field is vanishingly small compared with the local exchange field that comes from exchange and correlation interaction among the interacting Cr 3*d* orbitals. The recorded RIXS spectra reported here reveal clearly resolved Cr 3*d* intraorbital *dd* excitations that represent transitions between electronic levels that are heavily influenced by dynamic correlations and multiconfiguration effects. Our calculations taking into account the Cr 3*d* hybridization with the ligand valence states and the full multiplet structure due to intra-atomic and crystal field interactions in O_h and D_{3d} symmetry clearly reproduced the dichroic trend in experimental RIXS spectra.

DOI: 10.1103/PhysRevB.107.115148

I. INTRODUCTION

Over the last few years, two-dimensional (2D) van der Waals materials have spurred enormous interest due to their unique magnetic properties and potential in the development of multifunctional electronics and spintronics devices [1–5]. Among various 2D systems, the family of CrX_3 (X = Cl, Br, and I) has recently been at the center of widespread research in developing high-quality samples, from monolayer to bulk single crystals. Although ferromagnetism in semiconducting bulk CrI_3 has been known since the mid-twentieth century [6], recent experiments reveal layer-dependent magnetic phases [7,8]: from ferromagnetism in the monolayer to antiferromagnetism in the bilayer and back to ferromagnetism in the trilayer and bulk. This has been postulated to arise from competing interlayer and intralayer antiferromagnetic and ferromagnetic interactions, respectively [8]. According to Mermin-Wagner theory [9], in the absence of intrinsic anisotropy, long-range magnetic order is strongly suppressed in a 2D isotropic Heisenberg system due to spin fluctuation at a finite temperature. However, any deviation from a pure Heisenberg interaction, such as the influence of the magnetocrystalline anisotropy (MCA), would be able to stabilize a magnetically ordered state, which is most likely what happens in CrI_3 [10]. In CrI_3, the MCA energy is $\Delta E_{\mathrm{MCA}} \sim 0.5$ meV [11], a large value whose origin has been a topic of enormous interest in the past couple of years with continued debate. X-ray magnetic circular dichroism (XMCD) studies at Cr $L_{2,3}$ and I $M_{4,5}$ edges revealed strongly suppressed single-ion anisotropies of Cr 3*d* and I 5*p* states, whose energies are too small to explain the origin of ΔE_{MCA}.

*mahmoudhafiez@gmail.com

Despite this, there is a considerable spin-orbit coupling (SOC) strength (∼0.63 eV) in the I 5*p* state and strong Cr 3*d*–I 5*p* hybridization [12,13]. The I 5*p* state SOC strength primarily contributes to the MCA (in contrast to the much smaller SOC of Cr 3*d* ∼ 0.05 eV), either through the Cr 3*d*–I 5*p*–Cr 3*d* superexchange hopping or via substantial admixture of band states [14]. Superexchange in this material is stabilized by the inherent CrI_3 crystal structure constituting of trivalent Cr ions in an octahedral environment of I ions and the in-plane Cr-I-Cr bond angle ∼ 95°. In this configuration, according to the Goodenough-Kanamori-Anderson (GKA) rule, the Cr-Cr coupling is expected to be primarily ferromagnetic [15]. Therefore the origin of long-range ferromagnetism could be attributed to the high SOC of I 5*p* states mediating the anisotropic Cr 3*d*–I 5*p*–Cr 3*d* superexchange hopping through 95° in-plane Cr-I-Cr bond angle [16]. Recent theoretical results suggest that the magnetic interaction is not purely ferromagnetic; instead there is a competition between the ferromagnetic interaction and the antiferromagnetic interaction, which involve different Cr 3*d* orbitals [10,11,17,18]. Calculations also suggest a sizable contribution of the orbital-resolved components of Cr 3*d* states from nearest-neighbor interactions [19,20]. In monolayer CrI_3, recent electronic structure calculations reveal substantial exchange splitting of the spin-polarized Cr 3*d* t_{2g} and e_g states due to ferromagnetic Cr-I-Cr superexchange interaction [20]. However, the electronic structure of this (and similar) materials is complex, with expected competition from kinematic (band formation) effects and on-site Coulomb repulsion (e.g., as parametrized by the Hubbard *U*). It is expected that the Cr 3*d* interorbital interactions mediated by the I 5*p* orbital hold the key to understanding most electronic, magnetic, and transport properties of CrI_3 [21]. Therefore probing the Cr 3*d* orbital is indispensable for an in-depth understanding of the magnetic properties of CrI_3. To directly access the Cr 3*d* orbitals, we carried out resonant inelastic x-ray scattering (RIXS) studies at the Cr $L_{2,3}$ edge of bulk CrI_3 single-crystal samples with circularly polarized x rays. Soft x-ray RIXS, corresponding to the direct transition from Cr 2*p* core levels to the Cr 3*d* orbitals, allows us to study orbital (*dd*) excitations. In addition, magnetic circular dichroism (MCD) in RIXS enabled an in-depth understanding of magnetic interactions from the *dd* excitation which is also sensitive to the symmetry of the *d* orbitals. The experimental investigations are found to be well corroborated by electronic structure calculations.

II. EXPERIMENTAL AND THEORETICAL METHODS

Bulk CrI_3 single crystals were grown by chemical vapor transport, by reacting chromium powder (99.5%; Sigma-Aldrich) and anhydrous iodine beads (99.999%; same supplier) in a 1:3 ratio inside a glovebox with an argon atmosphere. Figures 1(a) and 1(b) show a scanning electron microscopy image of a CrI_3 single-crystal sample from the top and side, respectively, along with a schematic crystal structure shown at the bottom of each panel. The easily cleavable quality of the sample is clearly visible as multiple layers are observed particularly in Fig. 1(b), where the platelike crystal is bent to get a side view of the layers. Magnetization studies have been performed using a Quantum Design MPMS3 magnetometer with magnetic fields $\mu_0 H$ up t_p 7 T applied parallel and perpendicular to the crystallographic *c* axis, respectively. The calculations of the RIXS spectra of CrI_3 in this paper were performed in the framework of the Anderson impurity model (AIM) using the QUANTY software package (for detailed information, see Supplemental Material [22]). The spectra of Cr^{3+} were calculated considering the Cr 3*d* hybridization with the ligand valence states and the full multiplet structure due to intra-atomic and crystal field interactions. The Slater integrals $F^k(3d, 3d)$, $F^k(2p, 3d)$, and $G^k(2p, 3d)$ calculated for the Cr^{3+} ion were scaled down to 80% of their *ab initio* Hartree-Fock values. The calculations were done for O_h and D_{3d} symmetry. The crystal field parameters for the 3*d* shell were set to $10D_q = 1.55$ eV in the case of O_h symmetry and to $D_q = 0.155$ eV, $D_\sigma = -0.3$ eV, and $D_\tau = 0.0$ eV in the case of D_{3d} symmetry.

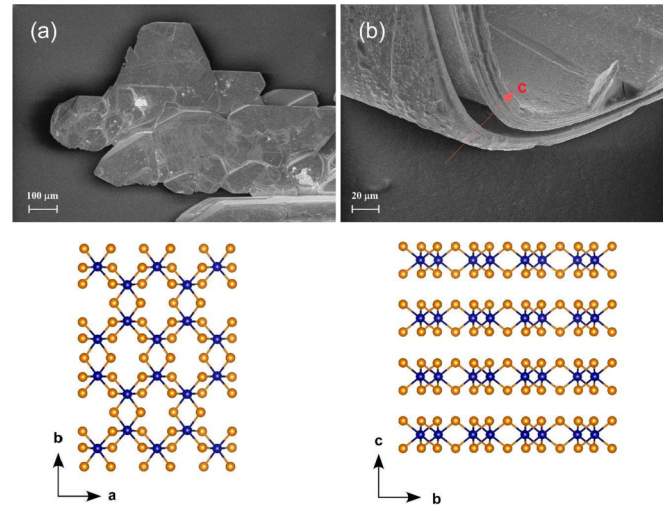

FIG. 1. Scanning electron microscope (SEM) image of CrI_3 single crystal from (a) the top and (b) the side and the corresponding crystal structures in the *ab* plane and along the *c* axis. The red arrow in the SEM image in (b) shows the *c* direction corresponding to the direction of CrI_3 layers stacking as shown schematically below.

III. RESULTS

Figure 2(a) shows the magnetization *M* vs magnetic field plots at 2 K and at two alignments of the magnetic field, $H \parallel c$ and $H \parallel ab$. While the saturation magnetizations M_s along the two directions are similar, there is a substantial difference in the saturation fields for $H \parallel c$ (H_c^s) and $H \parallel ab$ (H_{ab}^s). Therefore the anisotropy field is given by $\Delta\mu_0 H_s = \mu_0 H_{ab}^s - \mu_0 H_c^s \sim 3.16$ T, from which we deduce a magnetic anisotropy energy of ∼0.55 meV, in agreement with a previous report [11]. Figure 2(b) shows *M* vs temperature [$M(T)$] plots at an external magnetic field of 0.1 T applied parallel to the *c* axis and the *ab* plane. The out-of-plane (easy axis) spins will not completely polarize along the *ab* plane at a nominal field of 0.1 T due to MCA [see Fig. 2(a); a magnetic field of more than 3 T is required to overcome the MCA energy and polarize all the spins along the *ab* plane] [23]. However, the projections of the canted *c*-axis spins on the *ab* plane, at $\mu_0 H \parallel ab$ and 0.1 T, could be antiferromagnetic [AFM; bottom right inset in Fig. 2(b)], which explains the $M(T)$

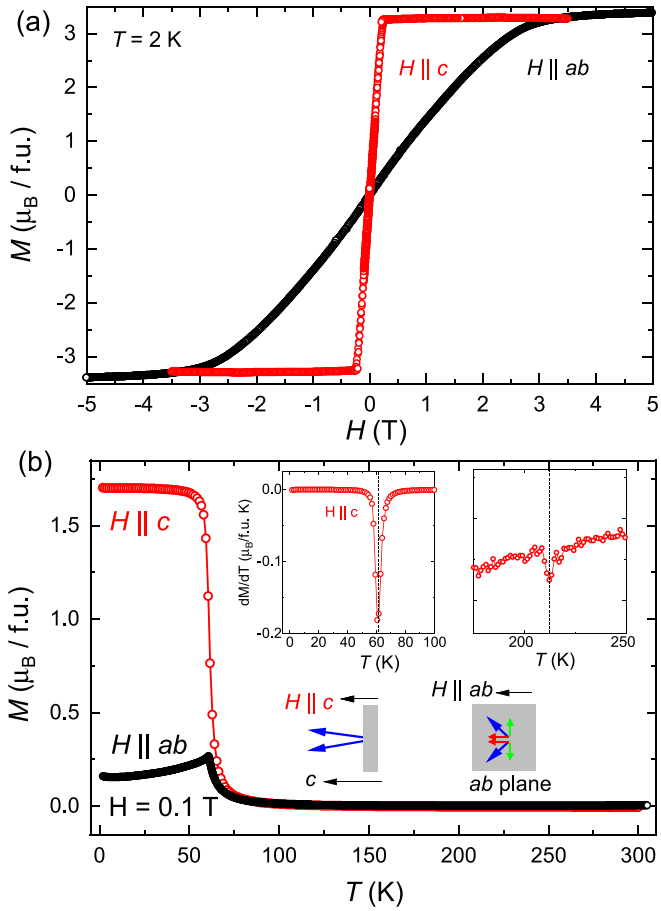

FIG. 2. (a) $M(\mu_0 H)$ measured at 2 K, and (b) $M(T)$ plots with applied dc magnetic field parallel to the c axis and to the ab plane. The top insets in (b) show the dM/dT plots to extract T_C and T_S. At an in-plane magnetic field ($\mu_0 H \parallel ab$: $H = 0.1$ T). The temperature derivative of M [top insets in Fig. 1(b)] gives a sharp peak at 61 K and a weak peak near 212.5 K, which are attributed to the FM to paramagnetic (PM) transition temperature (T_C) and phase transition from rhombohedral ($R\bar{3}$) to monoclinic ($C2/m$) crystal structure (T_S), respectively.

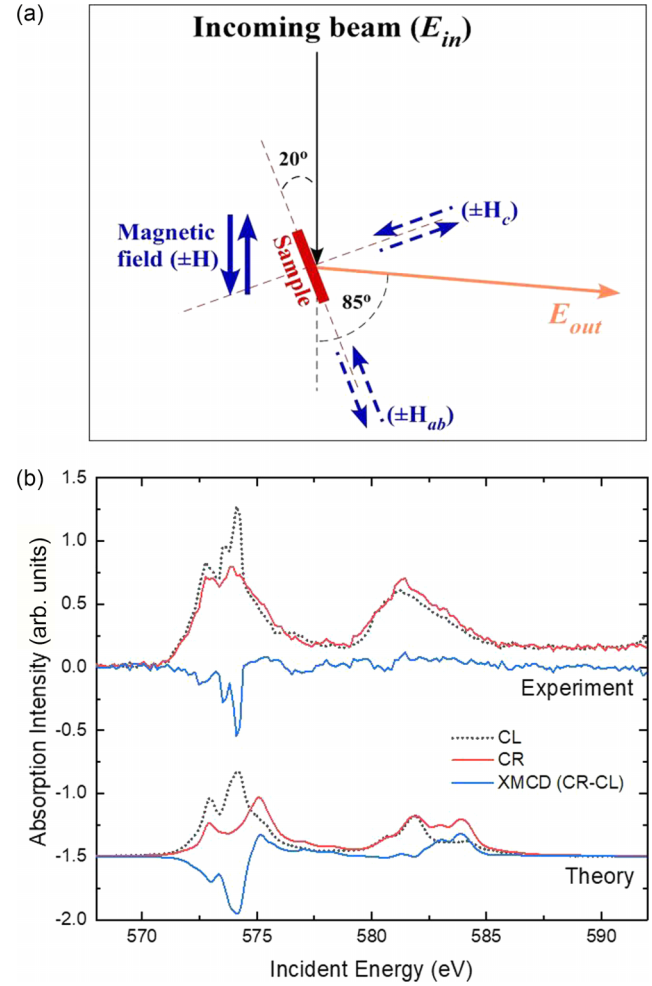

FIG. 3. (a) Schematic illustration of experimental geometry. The sample was illuminated with circularly polarized x-ray photons of energy E_{in} at 20° grazing to the sample surface. The scattered rays (E_{out}) were detected by the spectrometer fixed at 85° scattering angle. A magnetic field, $H = 0.5$ T, was applied parallel to the x rays, and H_c and H_{ab} are the components of H parallel to the c axis and ab plane, respectively. (b) Top: Cr $L_{3,2}$ XAS and XMCD spectra measured at 20 K and $+H$ magnetic field. Bottom: Calculated XAS and XMCD spectra. The inset shows the area under the energy loss region between 0.6 and 5 eV of the RIXS spectra.

line shape for $\mu_0 H \parallel ab$. Also, these in-plane spins are not collinear at a nominal magnetic field (0.1 T), which explains why at the lowest measured temperature (2 K) there is still a small but finite M. To probe the in-plane ferromagnetic (FM) interactions at a nominal in-plane magnetic field (above the $H \parallel c$ saturation field), we have carried out x-ray magnetic circular dichroism (XMCD) and RIXS studies at the Cr $L_{2,3}$ edge. Cr $L_{2,3}$-edge RIXS measurements were carried out at the SEXTANTS beamline [24,25] of the SOLEIL Synchrotron using the novel MAGELEC sample environment [26]. Left and right circular (CL and CR) polarized x rays of energy across the Cr $L_{2,3}$ edge (E_{in}) were focused at 20° grazing to the sample surface (ab plane) A schematic representation of the experimental geometry is presented in Fig. 3(a). A magnetic field, $H = 0.5$ T, was applied parallel to the incoming x-ray beam. Therefore the components of H along the c axis (H_c) and ab plane (H_{ab}) are 0.17 and 0.33 T, respectively. Measurements were carried out at 20 and 100 K, i.e., below and above the Curie temperature.

Figure 3(b) shows the Cr $L_{2,3}$-edge x-ray absorption spectra (XAS) and corresponding XMCD of a CrI_3 single-crystal sample at 20 K [ferromagnetic phase of rhombohedral ($R\bar{3}$) crystal structure]. XAS were recorded in the total electron yield mode with CL and CR polarized x rays. XMCD is the difference between the CR and CL polarized XAS as shown at the top of Fig. 3(b). The bottom of Fig. 3(b) shows the calculated XAS and XMCD spectra. Calculations involve using the multiplet of the ground state configuration together with corresponding quantum numbers (including S, L, and J) using QUANTY [27,28] (see Supplemental Material for details of the calculations) in the framework of the Anderson impurity model (with spins aligned parallel to the magnetic field, along the c axis). In the QUANTY calculations, parameters such as the crystal field splitting and the spin-orbit coupling are treated as adjustable parameters. The calculated XAS and XMCD

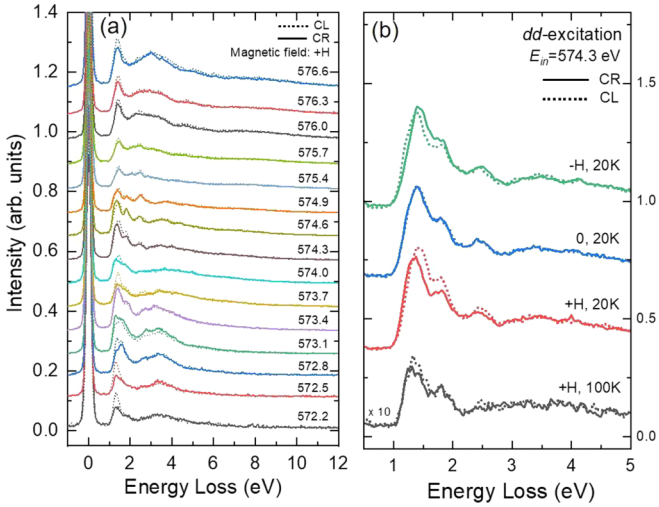

FIG. 4. (a) RIXS energy loss spectra at 20 K at various circularly polarized (CL and CR) excitation energies. $+H$ was the direction of the magnetic field. (b) MD in the elastic (left side of panel) and dd excitation (right side of panel) features at 20 K ($-H$, 0, and $+H$ magnetic fields) and 100 K ($+H$ magnetic field).

spectra, as shown at the bottom of Fig. 3(b), agree fairly well with the experimental data.

Figure 4(a) summarizes the RIXS energy loss spectra at various excitation energies (for CR and CL polarized x rays) mentioned alongside each spectrum. In a conventional RIXS process, a monochromatic beam of energy E_{in} is incident onto the sample, and one measures the energy distribution of the emitted radiation (E_{out}) converted into an energy loss ($E_{\text{in}} - E_{\text{out}}$) scale to determine any low-energy excitations of the system. The energy loss at 0 eV corresponds to the elastically scattered photons (where $E_{\text{in}} = E_{\text{out}}$), while other features correspond to dd excitations, charge transfer (CT), and Cr L_α fluorescence, in the order of increasing energy loss. For coherent dd and CT excitations [29,30], the energy losses are independent of incident energy and are also known as Raman-like losses. We identify the dd excitation features (1.45 ± 0.02, 1.75 ± 0.02, and 2.50 ± 0.05 eV) between 1 and 3 eV energy loss as shown in Fig. 4(a), and for better clarity we replot the RIXS spectrum at the resonance L_3 energy (574.3 eV) in Fig. 4(b). Above 575 eV excitation energy [Fig. 4(a)], the broad feature (between 2 and 5 eV) resembles the emission (L_α) from Cr $3d_{5/2}$ to $2p_{3/2}$ in addition to the buried dd and CT features. The broad feature in the RIXS spectra excited near the absorption threshold (near 572 eV) signifies the metal-ligand CT (3.50 ± 0.10 eV), which gets smeared out in intensity relative to the dd excitation features, near the resonant energy. The difference in intensities between the CL and CR RIXS features at 20 K, in particular at dd excitations, is clearly visible at resonant excitation and also at other excitation energies in Fig. 4(a). A clear contrast in the integrated intensities can also be observed in addition to the XMCD contrast in Fig. 2. Upon reversing the direction of the magnetic field (to $-H$), the CL and CR RIXS features in the dd excitation also switch their relative intensity depending on the light helicity, and at zero magnetic field their intensities are similar [Fig. 4(b)]. This behavior is direct evidence of magnetic dichroism (MD) in RIXS and is not an experimental artifact. Above T_C, at 100 K, we multiply the intensity by 10 to make it comparable to that at 20 K. Such a reduction in intensity above T_C is expected primarily due to the disordered orientation in the spin state, when the conductivity and crystal structure of CrI_3 remain similar at the two temperatures [31].

As discussed earlier in the present measurement geometry, the MD in RIXS is primarily due to the Cr spins parallel to the c axis. This is due to the fact that even at $H_c = 0.17$ T, the Cr spins parallel to the c axis are fully ferromagnetically saturated, in contrast to unsaturated in-plane Cr spins at $H_{ab} = 0.33$ T [see Fig. 2(a)]. However, at the nominal magnetic field, the in-plane spins can be antiferromagnetically oriented as already observed in Fig. 2(b). A similar situation is present in α-Fe_2O_3 [32], where the spin-flip excitations involving the e_g states were interpreted as the origin of anisotropic SOC, which was responsible for the Dzyaloshinskii-Moriya (DM) interaction. Although structurally Fe_2O_3 and CrI_3 are entirely different systems, one cannot neglect the fact that similar MDs in dd excitation are observed in these two systems, in addition to the coexistence of in-plane FM and AFM interactions. Therefore it may be worthwhile to consider the possibility that MD in dd excitation in CrI_3 could be due to spin-flip excitation. DM interaction may also be present in CrI_3, which is believed to be the origin of the spin gap at the Dirac point of spin-wave (SW) excitation spectra, observed in inelastic neutron scattering experiments [33]. Several calculations [20,33,34] showed that in the absence of DM interaction the origin of the spin gap cannot be explained, and the system would eventually be similar to a spin analog of graphene (spin-gap-less at the Dirac point). There is, however, a continued debate on the strength of DM interaction. A realistic estimation of DM interaction strength, by Kvashnin *et al.* [20], as compared with the Heisenberg exchange interaction, underestimates the spin-gap value, although it fairly accurately predicts the splitting in the Cr $3d$ orbital and corresponding spin-flip dd excitations (1.45, 1.75, and 2.50 eV). Kitaev interaction [35] and electron correlation [36] may also contribute to the origin of the spin gap in SW excitation. Recently, we found possible evidence of a complex magnetic spin-liquid-like state at high pressures and very low temperatures in a CrI_3 single crystal [37]. However, further investigations are required to quantify the roles of DM and Kitaev interactions, associated with the SOC strength, in accurately estimating the magnitude of the spin-gap and spin-flip dd excitations.

Importantly, we do not observe any significant peak shift or splitting between the RIXS spectra at 20 and 100 K. This demonstrates that the ferromagnetic superexchange interaction that is responsible for the interatomic exchange field is vanishingly small compared with the local exchange field that comes from intra-atomic exchange and correlation interaction among the interacting Cr $3d$ orbitals of a given site. The latter interaction is driven by local exchange interactions of the order of eV, which is clearly much larger than estimates of interatomic exchange which is on the meV level. Figures 5(a) and 5(b) plot the experimental RIXS map near the Cr L_3 region for CL and CR polarization, respectively, at 20 K. RIXS spectra at the Cr L_3 resonance excitation for CL and CR are shown in Fig. 5(c) [replot of Fig. 4(b) for $+H$ at 20 K]. For comparison, we plot the corresponding calculated RIXS

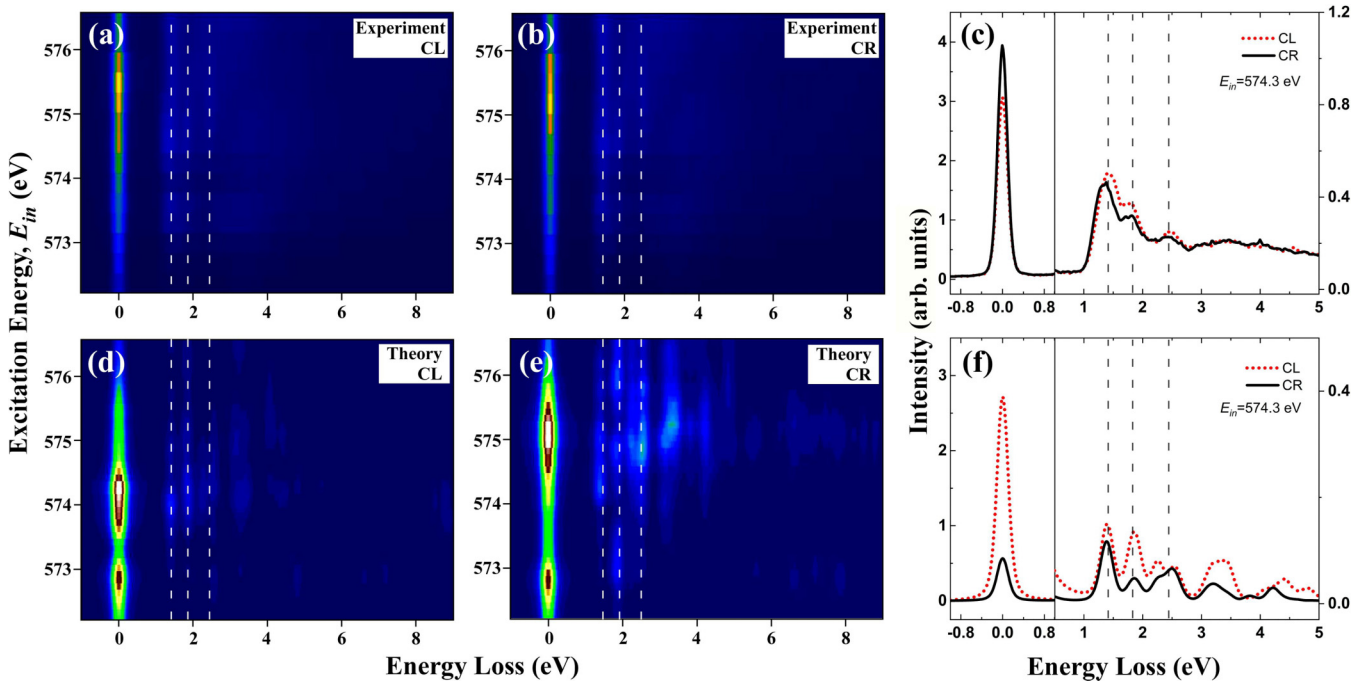

FIG. 5. Experimental RIXS maps measured at 20 K with (a) CL and (b) CR polarized x rays incident grazing to the sample surface and a magnetic field along the $+H$ direction. (c) Dichroic RIXS spectra at resonant excitation along the $+H$ direction. Calculated RIXS maps with (d) CL and (e) CR polarized x rays. (f) Line spectra at 574.3 eV excitation energy obtained from (d) and (e).

map in Figs. 5(d) and 5(e) and the line spectra at resonance L_3 excitation in Fig. 5(f). In the calculations, we did not consider the self-absorption effects and the possibility of reflections from the sample surface, which might lead to discrepancies between the experimental and theoretical dichroic elastic peak signal. We also note that the present experimental resolution (around 180 meV at the Cr L_3 edge) prohibits the occurrence of well-resolved peaks particularly above 2.5 eV, although the integrated spectral features match well with the calculations. The dichroism and the energy loss peak positions in the calculated spectra, considering a SOC in the system, fairly agree with those of the experiment. A dichroic signal can only be recovered in these types of calculations if spin-orbit effects are included (see Fig. S1 of the Supplemental Material). Therefore SOC plays a significant role and may also be responsible for the DM interaction when considering the projected in-plane FM spins in the in-plane AFM matrix at a nominal in-plane magnetic field. However, further calculations are necessary to explicitly understand and quantify the effects of DM and Kitaev interactions, which are based on SOC, on the orbital excitations in CrI_3 and the related family of 2D materials.

IV. CONCLUSION

To summarize, we find that our experimental data are in good agreement with the spectra calculated using a theoretical method that allows for multiconfiguration effects, when spin-orbit correlations are included (see Supplemental Material for more details [22]). For the spectroscopic features we note that a theory on the multiconfigurational level reproduces experimental observations with high precision. The investigation presented here demonstrates that the electronic structure of bulk CrI_3 (and most likely of its 2D sister compounds) is complex in the sense that dynamical electron correlations are important, meaning that the electronic structure signals multiconfiguration effects. This is signaled from both the ground state (magnetic moment) and spectroscopic, excited state properties. The recorded RIXS spectra here reveal clearly resolved Cr $3d$ intraorbital dd excitations that represent transitions between electronic levels heavily influenced by multiconfiguration effects. The MD observed in the dd excitations could reflect spin flip and, in conjunction with SOC, could support DM interaction as well, imparting tremendous interest in this and similar 2D materials for future investigations.

ACKNOWLEDGMENTS

The authors would like to thank Håkan Rensmo for the fruitful discussions. A.G. and M.A.-H. acknowledge financial support from the Carl Tryggers Foundation and the Swedish Research Council (VR) under Project No. 2018-05393. D.J.M. acknowledges support from SSF Grant No. RIF14-0064. O.E. acknowledges financial support from the Knut and Alice Wallenberg Foundation, eSSENCE, the Swedish Research Council (VR), and the Foundation for Strategic Research (SSF). O.E. and P.T. acknowledge support from ERC synergy Grant No. 854843-FASTCORR. Y.K. acknowledges support from VR (Project No. 2019-03569) and the Göran Gustafsson Foundation. Support from the P220 program Project No. 075-15-2021-604 is acknowledged. The computations were enabled by resources provided by the Swedish National Infrastructure for Computing (SNIC) at the National Supercomputer Centre (NSC) partially funded by the Swedish Research Council through Grant Agreement No. 2018-05973. D.P. acknowledges

support from the Swedish Research Council under Project No. 2020-00681. T.S. acknowledges financial support from the Swedish Research Council (VR Grants No. 2017-05030 and No. 2021-03675). M.H. acknowledges support by the European Union's Horizon 2020 Research and Innovation Programme, under Grant Agreement No. 824109 (European Microkelvin Platform). Work at Heidelberg has been supported by BMBF via the project SpinFun (13XP5088) and by Deutsche Forschungsgemeinschaft (DFG) under Germany's Excellence Strategy EXC2181/1-390900948 (the Heidelberg STRUCTURES Excellence Cluster). M.V.K. acknowledges support from ERC Grant No. 101002772-SPINNER.

[1] K. S. Novoselov, A. Mishchenko, A. Carvalho, and A. H. Castro Neto, 2D materials and van der Waals heterostructures, Science **353**, aac9439 (2016).

[2] C. Gong, L. Li, Z. Li, H. Ji, A. Stern, Y. Xia, T. Cao, W. Bao, C. Wang, Y. Wang, Z. Q. Qiu, R. J. Cava, S. G. Louie, J. Xia, and X. Zhang, Discovery of intrinsic ferromagnetism in two-dimensional van der Waals crystals, Nature (London) **546**, 265 (2017).

[3] M. Bonilla, S. Kolekar, Y. Ma, H. C. Diaz, V. Kalappattil, R. Das, T. Eggers, H. R. Gutierrez, M. H. Phan, and M. Batzill, Strong room-temperature ferromagnetism in VSe_2 monolayers on van der Waals substrates, Nat. Nanotechnol. **13**, 289 (2018).

[4] A. Majumdar, D. Vangennep, J. Brisbois, D. Chareev, A. V. Sadakov, A. S. Usoltsev, M. Mito, A. V. Silhanek, T. Sarkar, A. Hassan, O. Karis, R. Ahuja, and M. Abdel-Hafiez, Interplay of charge density wave and multiband superconductivity in layered quasi-two-dimensional materials: The case of 2H-NbS_2 and 2H-$NbSe_2$, Phys. Rev. Mater. **4**, 084005 (2020).

[5] Y. Kvashnin, D. Vangennep, M. Mito, S. A. Medvedev, R. Thiyagarajan, O. Karis, A. N. Vasiliev, O. Eriksson, and M. Abdel-Hafiez, Coexistence of Superconductivity and Charge Density Waves in Tantalum Disulfide: Experiment and Theory, Phys. Rev. Lett. **125**, 186401 (2020).

[6] J. F. Dillon Jr. and C. E. Olson, Magnetization, resonance, and optical properties of the ferromagnet CrI_3, J. Appl. Phys. **36**, 1259 (1965).

[7] B. Huang, G. Clark, E. Navarro-Moratalla, D. R. Klein, R. Cheng, K. L. Seyler, Di. Zhong, E. Schmidgall, M. A. McGuire, D. H. Cobden, W. Yao, D. Xiao, P. Jarillo-Herrero, and X. Xu, Layer-dependent ferromagnetism in a van der Waals crystal down to the monolayer limit, Nature (London) **546**, 270 (2017).

[8] L. Thiel, Z. Wang, M. A. Tschudin, D. Rohner, I. Gutiérrez-Lezama, N. Ubrig, M. Gibertini, E. Giannini, A. F. Morpurgo, and P. Maletinsky, Probing magnetism in 2D materials at the nanoscale with single-spin microscopy, Science **364**, 973 (2019).

[9] N. D. Mermin and H. Wagner, Absence of Ferromagnetism or Antiferromagnetism in One- or Two-Dimensional Isotropic Heisenberg Models, Phys. Rev. Lett. **17**, 1133 (1966).

[10] O. Besbes, S. Nikolaev, N. Meskini, and I. Solovyev, Microscopic origin of ferromagnetism in the trihalides $CrCl_3$ and CrI_3, Phys. Rev. B **99**, 104432 (2019).

[11] D. H. Kim, K. Kim, K. T. Ko, J. Seo, J. S. Kim, T. H. Jang, Y. Kim, J. Y. Kim, S. W. Cheong, and J. H. Park, Giant Magnetic Anisotropy Induced by Ligand *LS* Coupling in Layered Cr Compounds, Phys. Rev. Lett. **122**, 207201 (2019).

[12] J. L. Lado and J. Fernández-Rossier, On the origin of magnetic anisotropy in two dimensional CrI_3, 2D Mater. **4**, 035002 (2017).

[13] A. Frisk, L. B. Duffy, S. Zhang, G. van der Laan, and T. Hesjedal, Magnetic x-ray spectroscopy of two-dimensional CrI_3 layers, Mater. Lett. **232**, 5 (2018).

[14] C. Andersson, B. Sanyal, O. Eriksson, L. Nordström, O. Karis, D. Arvanitis, T. Konishi, E. Holub-Krappe, and J. H. Dunn, Influence of Ligand States on the Relationship between Orbital Moment and Magnetocrystalline Anisotropy, Phys. Rev. Lett. **99**, 177207 (2007).

[15] J. Kanamori, Superexchange interaction and symmetry properties of electron orbitals, J. Phys. Chem. Solids **10**, 87 (1959).

[16] L. Webster and J. A. Yan, Strain-tunable magnetic anisotropy in monolayer $CrCl_3$, $CrBr_3$, and CrI_3, Phys. Rev. B **98**, 144411 (2018).

[17] S. W. Jang, M. Y. Jeong, H. Yoon, S. Ryee, and M. J. Han, Microscopic understanding of magnetic interactions in bilayer CrI_3, Phys. Rev. Mater. **3**, 031001(R) (2019).

[18] J. Arneth, M. Jonak, S. Spachmann, M. Abdel-Hafiez, Y. O. Kvashnin, and R. Klingeler, Uniaxial pressure effects in the two-dimensional van der Waals ferromagnet CrI_3, Phys. Rev. B **105**, L060404 (2022).

[19] I. V. Kashin, V. V. Mazurenko, M. I. Katsnelson, and A. N. Rudenko, Orbitally-resolved ferromagnetism of monolayer CrI_3, 2D Mater. **7**, 025036 (2020).

[20] Y. O. Kvashnin, A. Bergman, A. I. Lichtenstein, and M. I. Katsnelson, Relativistic exchange interactions in CrX_3 (X = Cl, Br, I) monolayers, Phys. Rev. B **102**, 115162 (2020).

[21] Y. Liu and C. Petrovic, Three-dimensional magnetic critical behavior in CrI_3, Phys. Rev. B **97**, 014420 (2018).

[22] See Supplemental Material at http://link.aps.org/supplemental/10.1103/PhysRevB.107.115148 for calculation details and supporting results.

[23] M. Jonak, E. Walendy, J. Arneth, M. Abdel-Hafiez, and R. Klingeler, Low-energy magnon excitations and emerging anisotropic nature of short-range order in CrI_3, Phys. Rev. B **106**, 214412 (2022).

[24] S. G. Chiuzbăian, C. F. Hague, A. Avila, R. Delaunay, N. Jaouen, M. Sacchi, F. Polack, M. Thomasset, B. Lagarde, A. Nicolaou, S. Brignolo, C. Baumier, J. Lüning, and J. M. Mariot, Design and performance of AERHA, a high acceptance high resolution soft x-ray spectrometer, Rev. Sci. Instrum. **85**, 043108 (2014).

[25] M. Sacchi, N. Jaouen, H. Popescu, R. Gaudemer, J. M. Tonnerre, S. G. Chiuzbaian, C. F. Hague, A. Delmotte, J. M. Dubuisson, G. Cauchon, B. Lagarde, and F. Polack, The SEXTANTS beamline at SOLEIL: A new facility for elastic, inelastic and coherent scattering of soft X-rays, in *Proceedings of the 11th International Conference on Synchrotron Radiation Instrumentation (SRI 2012) 9–13 July 2012, Lyon, France*, Journal of Physics: Conference Series Vol. 425 (Institute of Physics, London, 2013), p. 072018.

[26] A. Nicolaou, V. Pinty, F. Marteau, J.-M. Dubuisson, P. Rommeluere, E. Dupuy, F. Bouvet, D. Corruble, C. Såthe, M. Agåker, J.-E. Rubensson, M. Nouna, P. Goy, S. Lorcy, and C. Herbeaux, MAGELEC: A unique sample environment for performing RIXS under electric and magnetic

field, in *Proceedings of the 15th SOLEIL Users' Meeting* (Synchrotron SOLEIL, Saint-Aubin, France, 2020), p. PO-10, https://www.synchrotron-soleil.fr/en/file/12497/download?token=FX_uM-Vm.

[27] M. W. Haverkort, M. Zwierzycki, and O. K. Andersen, Multiplet ligand-field theory using Wannier orbitals, Phys. Rev. B **85**, 165113 (2012).

[28] S. Johan, Impurity model, 2018, https://github.com/JohanSchott/ImpurityModel.

[29] M. A. McGuire, H. Dixit, V. R. Cooper, and B. C. Sales, Coupling of crystal structure and magnetism in the layered, ferromagnetic insulator CrI_3, Chem. Mater. **27**, 612 (2015).

[30] L. J. P. Ament, M. Van Veenendaal, T. P. Devereaux, J. P. Hill, and J. Van Den Brink, Resonant inelastic x-ray scattering studies of elementary excitations, Rev. Mod. Phys. **83**, 705 (2011).

[31] S. Mondal, M. Kannan, M. Das, L. Govindaraj, R. Singha, B. Satpati, S. Arumugam, and P. Mandal, Effect of hydrostatic pressure on ferromagnetism in two-dimensional CrI_3, Phys. Rev. B **99**, 180407(R) (2019).

[32] J. Miyawaki, S. Suga, H. Fujiwara, M. Urasaki, H. Ikeno, H. Niwa, H. Kiuchi, and Y. Harada, Dzyaloshinskii-Moriya interaction in α-Fe_2O_3 measured by magnetic circular dichroism in resonant inelastic soft x-ray scattering, Phys. Rev. B **96**, 214420 (2017).

[33] L. Chen, J.-H. Chung, M. B. Stone, A. I. Kolesnikov, B. Winn, V. O. Garlea, D. L. Abernathy, B. Gao, M. Augustin, E. J. G. Santos, and P. Dai, Magnetic Field Effect on Topological Spin Excitations in CrI_3, Phys. Rev. X **11**, 031047 (2021).

[34] L. Chen, J. H. Chung, B. Gao, T. Chen, M. B. Stone, A. I. Kolesnikov, Q. Huang, and P. Dai, Topological Spin Excitations in Honeycomb Ferromagnet CrI_3, Phys. Rev. X **8**, 041028 (2018).

[35] I. Lee, F. G. Utermohlen, D. Weber, K. Hwang, C. Zhang, J. Van Tol, J. E. Goldberger, N. Trivedi, and P. C. Hammel, Fundamental Spin Interactions Underlying the Magnetic Anisotropy in the Kitaev Ferromagnet CrI_3, Phys. Rev. Lett. **124**, 017201 (2020).

[36] L. Ke and M. I. Katsnelson, Electron correlation effects on exchange interactions and spin excitations in 2D van der Waals materials, npj Comput. Mater. **7**, 4 (2021).

[37] A. Ghosh, D. Singh, Q. Mu, Y. Kvashnin, G. Haider, M. Jonak, D. Chareev, T. Aramaki, S. A. Medvedev, R. Klingeler, M. Mito, E. H. Abdul-Hafidh, J. Vejpravova, M. Kalbàč, R. Ahuja, O. Eriksson, and M. Abdel-Hafiez, Exotic magnetic and electronic properties of layered CrI_3 single crystals under high pressure, Phys. Rev. B **105**, L081104 (2022).